ARTICLE

BIOTECHNOLOGY and BIOENGINEERING

Kinetic Responses of *Dunaliella* in Moving Fluids

Ahammed Anwar Chengala,[1] Miki Hondzo,[1] Dan Troolin,[2] Paul A Lefebvre[3]

[1]St. Anthony Falls Laboratory, Department of Civil Engineering, University of Minnesota, 2 Third Ave SE, Minneapolis, Minnesota 55414; telephone: 612-625-0053; fax: 612-624-4398; e-mail: mhondzo@umn.edu

[2]TSI Incorporated, 500 Cardigan Road, Shoreview, Minnesota 55126

[3]Department of Plant Biology, University of Minnesota, St. Paul, Minnesota 55108

Received 2 December 2009; revision received 13 March 2010; accepted 12 April 2010

Published online 26 April 2010 in Wiley InterScience (www.interscience.wiley.com). DOI 10.1002/bit.22774

ABSTRACT: The objective of this work was to quantify the kinetic behavior of *Dunaliella primolecta* (*D. primolecta*) subjected to controlled fluid flow under laboratory conditions. In situ velocities of *D. primolecta* were quantified by micron-resolution particle image velocimetry and particle tracking velocimetry. Experiments were performed under a range of velocity gradients and corresponding energy dissipation levels at microscopic scales similar to the energy dissipation levels of natural aquatic ecosystems. An average swimming velocity of *D. primolecta* in a stagnant fluid was 41 μm/s without a preferential flow direction. In a moving fluid, the sample population velocities of *D. primolecta* follow a log-normal distribution. The variability of sample population velocities was maximal at the highest fluid flow velocity in the channel. Local fluid velocity gradients inhibited the accrual of *D. primolecta* by twofold 5 days after the initiation of the experiment in comparison to the non-moving fluid control experiment.

Biotechnol. Bioeng. 2010;107: 65–75.

KEYWORDS: algae; *Dunaliella primolecta*; velocity; fluid flow; energy dissipation

Introduction

Dunaliella is a motile, bi-flagellated, cell-wall-less, unicellular green alga (belonging to the class of Chlorophyceae) whose cell size ranges from 9 to 17 μm. *Dunaliella* thrive in media containing extremely wide range of salt concentrations ranging from 0.1 to 5 M NaCl (Avron, 1992), and if grown under proper conditions, *Dunaliella* can accumulate appreciable amount of cartenoids (β-carotene), (Ben-Amotz et al., 1991; Schlipalius, 1991), glycerol (Ben-Amotz and Avron, 1982; Thakur and Kumar, 1998), and lipids (Tornabene et al., 1980; Vanitha et al., 2007). *Dunaliella* is relatively easy to continuously culture in a laboratory and have higher resistance to various environmental conditions compared to other species of algae (Aizawa and Miyachi, 1992). According to Ben-Amotz et al., (1991), *Dunaliella* strains are probably the most successful microalgae in mass cultivation, mainly due to their ability to survive in high saline environments characterized by extreme range of ecological adaptability (low temperatures, low pH, high irradiance, etc.), which reduces the number of competitors and predators. *Dunaliella* contain lipids and fatty acids as membrane components, storage products, metabolites and sources of energy.

Dunaliella has been found to be one of the richest natural sources of β-carotene (Hejazi and Wijffels, 2003; Raja et al., 2007; Zhu and Jiang, 2008). Under suitable conditions, *Dunaliella* can accumulate up to 10% of the dry cell weight of β-carotene (Loeblich, 1974; Jin and Melis, 2003). β-carotene is an orange pigment which has a wide range of applications in pharmaceutical industry, food, cosmetic, and as a coloring agent. *Dunaliella* contain 9-*cis*-β-carotene, which is up to ten times stronger at preventing cancer than ordinary β-carotene (Hieber et al., 2000). Production of β-carotene from natural sources has been of growing concern due to its increasing demand commercially (Lamers et al., 2008). Another major bi-product from *Dunaliella* harvest is glycerol (Mishra et al., 2008; Thakur et al., 2000). Glycerol is a colorless, viscous organic chemical widely used as a feedstock for the production of various chemicals and has found wide range of applications in the pharmaceutical, medical, cosmetic, leather and textile industries. More than 50% of the dry weight of *Dunaliella* may be glycerol depending on the salt concentrations in the growth medium (Ben-Amotz et al., 1982). Glycerol and β-carotene are the major products of *Dunaliella* suitable for commercial utilization. The commercial cultivation of Dunaliella for the production of β-carotene and glycerol throughout the world is now one of the success stories of halophile

Correspondence to: Miki Hondzo

Contract grant sponsor: National Center for Earth-surface Dynamics (NCED)
Contract grant sponsor: Minnesota Futures Grant

biotechnology (Ben-Amotz, 1980; Borowitzka et al., 1984), although it is economically less feasible due to the lack of advancement in biotechnological operations (Agarwal, 1990; Hadi et al., 2008).

An increasing demand for an alternative source of fuel for the ever depleting petroleum based fuels has been a widely discussed topic around the globe. It has been reported that the energy demand for transportation worldwide will double by the year 2020 (EIO report, 1999). Biodiesel obtained from natural sources is a very good alternative for petroleum based fuels since it is highly bio-degradable, renewable, non-toxic (particulate emissions are low) and carbon neutral. Algal species of *Dunaliella* have been found to have a promising economic potential to produce biodiesel from micro-algae (Gouveia and Oliveira, 2009). *D. primolecta* is one of the leading candidates in this endeavor because of its ability to produce lipids (triglycerides) that are suitable for direct use as an oil feedstock for the production of biodiesel. *D. primolecta* has been reported to have a lipid content of about 23% of its total body weight (Chisti, 2007) which makes it very promising for the biodiesel extraction.

The concept of using microalgae for sustainable feedstock production will be beneficial to the society if we are capable of culturing specific algae at large scales. Open ponds with mechanical mixing devices have been the major aquatic system explored for mass culture of microalgae. While the adaptive responses of *Dunaliella* to a variety of environmental conditions including temperature, light, salinity, and nutrient concentrations (Cowan et al., 1992; Chen and Jiang, 2009; Haghjou et al., 2009) have been reported, the kinetic responses of *Dunaliella* to fluid flow has not been investigated. In this study we report the kinetic behavior of *Dunaliella* at the cell scale under a variety of fluid flow conditions. Laboratory measurements were conducted under fluid flow energy dissipation levels reported in shallow lakes, wetlands, and ponds.

Materials and Methods

Culture Preparation

Strains of *D. primolecta* were obtained from UTEX, the culture collection of algae (University of Texas at Austin, USA), and were grown using the Erdschreiber's medium (Tompkins et al., 1995). A 500 mL of fresh culture was maintained at room temperature under cool white fluorescent light on a C1 platform shaker (New Brunswick Scientific Co., Inc., Edison, NJ) for a period of 14 days during which *D. primolecta* grow to its full size (~11 μm). Alternatively, *D. primolecta,* being a good swimmer, culture can be grown without the shaker by mixing them occasionally (twice a day) by hand. For each experimental run at specified Re, a 5 mL of culture was used in the experimental channel. The total duration of experiments lasted about 3 h.

Experimental Setup

A micro-particle image velocimetry (micro-PIV) system developed by TSI Inc. (Shoreview, MN) was used for the velocity quantification of *D. primolecta* cells and fluid flow in the experimental channel. The setup consists of an inverted microscope equipped with an epi-fluorescence filter cube, a double frame CCD camera (PIVCAM 14-10), a light-guide, a light source (Pulsed Nd:YAG laser and halogen lamp are used here), and a syringe pump (NE-500 model, New Era Pump Systems, Inc., Farmingdale, NY; Fig. 1). A light source illuminates the particles in the flow channel and is imaged through the microscopic objective onto the CCD camera. An optical filter cube consists of a dichromatic mirror and an emission filter and is used to separate the scattered fluorescent light from the illumination light. The dichromatic mirror has a coating that transmits the fluorescent emission wavelengths and reflects the laser wavelength. The working principle consists of illuminating particles in the flow using the light source. The measurement plane is defined by the depth of focus of the microscope objective; in-focus particles are measured and out-of-focus particles with a weak signal are not. Image pairs are captured using the camera separated by a short time interval. The average displacement of a group of particles is mapped by correlation (cross-correlation) of two consecutive images and is processed with analyzing software to obtain the velocity vector map.

The fluid flow channel was placed on the universal stage holder of the microscope. Fluorescent particles were used to seed the flow for the fluid flow analysis. Cultured *D. primolecta* were used as seeding particles for algal analysis. For the non-moving fluid experiment, that is, stagnant flow, no fluid flow was passed through the syringe pump thereby allowing *D. primolecta* cells to move freely and independently. For moving fluid flow measurements,

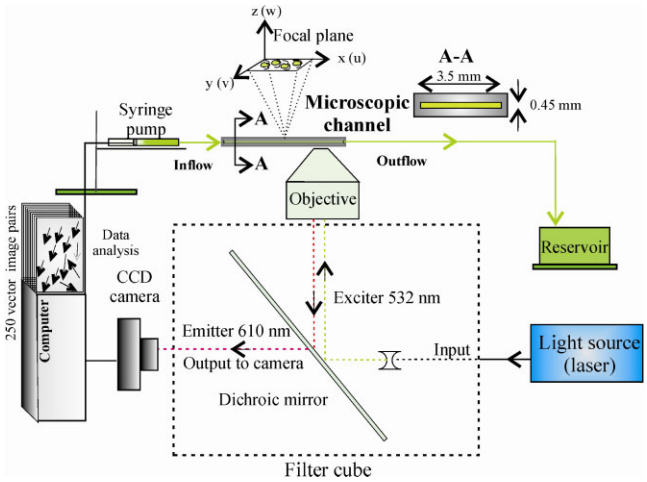

Figure 1. Schematic diagram illustrating the micro-PIV setup. [Color figure can be seen in the online version of this article, available at www.interscience.wiley.com.]

different flow rates were supplied through the computer-controlled syringe pump. The flow rates were chosen based on the fractions of swimming velocity of *D. primolecta* in stagnant fluid (e.g., 12.5%, 25%, etc. of the velocity). The seeded flow images were captured using a 10X objective and algal flow images were captured using a 4X objective of the microscope using the double frame CCD camera with 1,376 × 1,024 pixel resolution. The field of view for algal flow was 1.43 mm in the streamwise direction and 1.06 mm in the spanwise direction. For seeded flow it was 0.42 mm in the streamwise direction and 0.4 mm in the spanwise direction. A set of 250 double frame image pairs were recorded for both the algal and seeded flow with different flow rates with the timing between each frame (ΔT) adjusted to have a particle displacement of approximately 8–10 pixels. Typical value of ΔT for stagnant algal flow was 0.5 s and for moving flows (seeded and algal) it varied from 0.15 to 0.55 s depending on the flow rate. The recorded images were analyzed using the micro-PIV for fluid flow and Particle Tracking Velocimetry (PTV) for algal flow. For seeded flow, fluorescent particles appeared as white spots on a dark background while for the algal flow, *D. primolecta* cells appeared as dark spots on a bright background. Figure 2A shows a single frame image of *D. primolecta* cells in a stagnant fluid. A set of three experimental runs were repeated for each flow rate under identical experimental conditions. Under identical flow rate, no appreciable difference in mean velocities was observed. An independent set of experiments was also conducted by using a halogen lamp as a light source in the flow channel instead of the pulsing laser. The results demonstrated 1–2% difference in the velocities of *Dunaliella*. For each experiment, fresh culture of *Dunaliella* was transferred in the experimental channel. *Dunaliella* cells were never exposed longer than 60 s to the laser light in the channel for each independent experiment.

Seeding Particles

Fluid in the experimental channel was seeded with 1 μm diameter red dye-impregnated PSL (Polystyrene Latex) fluorescent particles (density of 1.05 g/cm^3) obtained from TSI Inc. and manufactured by Duke Scientific Corporation (Palo Alto, California). The peak excitation wavelength of the seeding particles is 542 nm and the emission peak is 612 nm. Distilled water mixed with the suspended fluorescent particle solution in the ratio of 10:1 was used as the working fluid. The velocity of the fluorescent seeding particles obtained through micro-PIV was taken as a reference velocity which was subtracted from the observed *Dunaliella* velocities. The net velocities of *Dunaliella* were acquired by PTV in which the fluid was not seeded by fluorescent particles, but rather, the individual cells of *Dunaliella* were visualized as the tracer particles. The *Dunaliella* do not fluoresce, so a fluorescent background was used to image the particles as dark spots on a bright background.

Flow Channel

Fluid flow channel was fabricated using PDMS (polydimethylsiloxane) having a rectangular cross-section with a depth of 0.45 mm and a width of 3.5 mm (Fig. 1). The length of the channel approximately measured 35 mm. The fluid in the channel was directed from the inlet of the channel using the syringe pump. The computer-controlled pump enable repeatability of experiments with algae and without algae at a specified fluid flow in the channel. All the measurements were taken at a vertical distance of 1/4th the channel depth from the channel bed (∼0.1 mm) and middle half of the channel (to avoid wall effects on *Dunaliella* swimming) close to the outlet of the channel after the flow was developed in the channel.

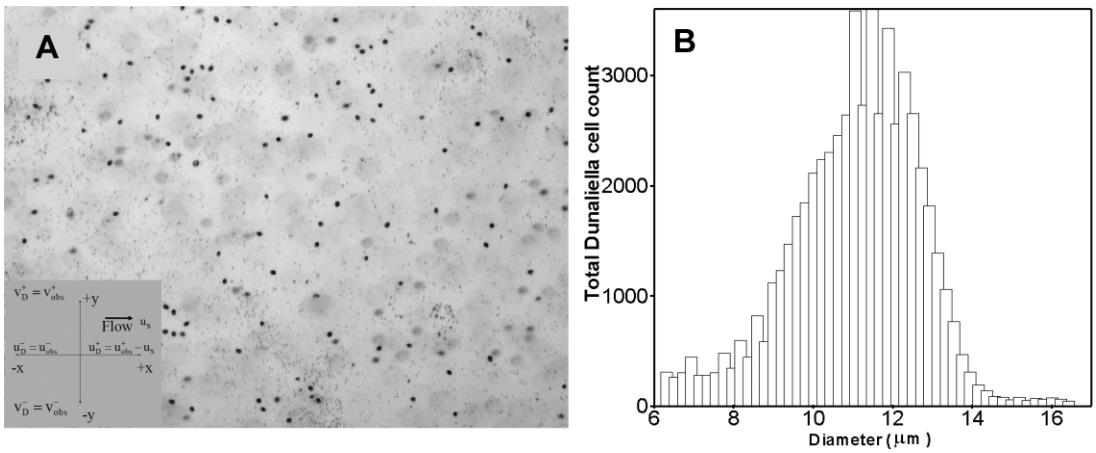

Figure 2. **A**: Depicts a single frame image of *D. primolecta* cells in the micro-channel in a stagnant fluid (captured using 4X objective of the microscope). *D. primolecta* cells appear as dark spots against a bright background. The field of view of the capture is 1.45 mm × 1.06 mm. **B**: The histogram plot of *D. primolecta* cells observed in a stagnant fluid. An average cell diameter of about 11 μm was observed.

PIV Versus PTV Analysis

Instantaneous velocity measurements are obtained for micron scale fluidic devices using micro-PIV analysis (e.g., Meinhart et al., 1999; Santiago et al., 1998). PTV analysis on the other hand, tracks the individual particles in the flow for obtaining instantaneous velocities. The main difference between micro-PIV and PTV analyses lies in the fact that the velocity obtained using micro-PIV is the velocity of all the particles averaged over an interrogation window (an image is broken down into a number of tiles called interrogation windows) where as the velocity obtained using PTV is the velocity of each individual particle in an interrogation window. The density of seeded particles is easily controllable in the interrogation window and hence fluid flow analysis was conducted by micro-PIV. PTV analysis was applied for algal velocity measurements for two reasons: the number density of algae was relatively low, and algae movements are independent, meaning that two algae next to each other can, and often do, move in completely different directions. Since micro-PIV and PTV generate advective velocity for the fluid flow under observation, the net *Dunaliella* velocity at a specified fluid flow, for varying flow rates (moving flows) were obtained by subtracting the seeded velocity at the corresponding flow rate.

Fluid Flow Analysis

The velocity vectors of fluid flow and algae were obtained using Insight3G software (TSI Inc.). For fluorescent seeded flow, images were processed using 64×64 pixel interrogation window with a recursive Nyquist grid algorithm, fast Fourier transform (FFT) correlator and bi-linear peak engine. Post-processing was done to remove and replace bad vectors which accounted for less than 5% of the resultant velocity vectors. This micro-PIV analysis was done for all flow rates to obtain seeded fluid flow velocities. For algal flow, all the image intensities were inverted to convert dark spots (*D. primolecta* cells appear as dark spots, Fig. 2A) to bright spots. A minimum intensity image was created by scanning each image in the set and obtaining the minimum pixel intensity at every location. This minimum intensity image was then subtracted from every image in the sequence, accentuating the particle images and diminishing the effect of constant sources of illumination such as background intensity, out of focus particles, and noise. This procedure was performed independently for the first and second frames to account for slight differences in the laser illumination. The subtracted images were used for PTV analysis. PTV involves selecting several parameters, namely, the maximum particle displacement between image frame based on *Dunaliella* movement, the intensity threshold value to determine the particles of interest (this helps to remove some speckles that still remain after background subtraction), the maximum size difference of a tracked particle from one frame to the next, and the minimum and maximum particle size. All the numbers provided for above descriptions were chosen based on the particular run (flow rate) which varied for different flow rates. The analysis was done for all flow rates to obtain observed *Dunaliella* velocities. For all the flow rates where *Dunaliella* had control over the flow, the observed *Dunaliella* velocities were higher than the seeded flow velocities for the corresponding flow rate. Net *Dunaliella* velocities were obtained by subtracting the seeded velocities from the observed *Dunaliella* velocities.

Flow Measurements

The seeded fluid flow velocities (Fig. 3A) and *Dunaliella* (algal) velocities (Fig. 3B and C) in the x–y plane were obtained from the instantaneous velocity vector maps using micro-PIV and PTV analysis, respectively. For algal flow analysis (Fig. 2A), the longitudinal components of velocity include (a) observed *Dunaliella* moving in the x-direction of flow (u^+_{obs}), and (b) observed *Dunaliella* moving opposite to the x-direction of flow (u^-_{obs}). The perpendicular components of velocity include (a) observed *Dunaliella* moving perpendicular the flow in the positive y-direction (v^+_{obs}), and (b) observed *Dunaliella* moving perpendicular to the flow in the negative y-direction (v^-_{obs}). For seeded flow analysis, the velocity component includes the longitudinal component of velocity in the flow direction or seeded fluid flow velocity (u_s). The perpendicular component of fluid flow velocity was zero since the flow was unidirectional driven by the syringe pump. The net velocity of *Dunaliella* cells in the longitudinal (x-flow) direction is denoted by u_D and the net velocity of *Dunaliella* cells in the perpendicular (y) direction is denoted by v_D. The value of u_D refers to the positive and negative velocities of *Dunaliella* as cells could move in both ($+$x and $-$x) directions. Similarly, The value of v_D refers to the positive and negative velocities of *Dunaliella* as cells could move in both ($+$y and $-$y) directions.

The net velocities of *Dunaliella* in the positive x-flow direction (u^+_D) were calculated for all flow rates as

$$u^+_D = u^+_{obs} - u_s \tag{1}$$

The net velocities of *Dunaliella* opposite (negative) to x-flow direction (u^-_D) were calculated for all flow rates as

$$v_D = v^+_{obs} = v^-_{obs} \tag{2}$$

Since the fluid flow was uni-directional (only in the positive x-flow direction), the net velocities of *Dunaliella* perpendicular to the flow in the positive y-direction of flow (v^+_D) was calculated for all flow rates as

$$v^+_D = v^+_{obs} \tag{3}$$

The net velocities of *Dunaliella* perpendicular to the flow in the negative y-direction of flow (v^-_D) was calculated for all

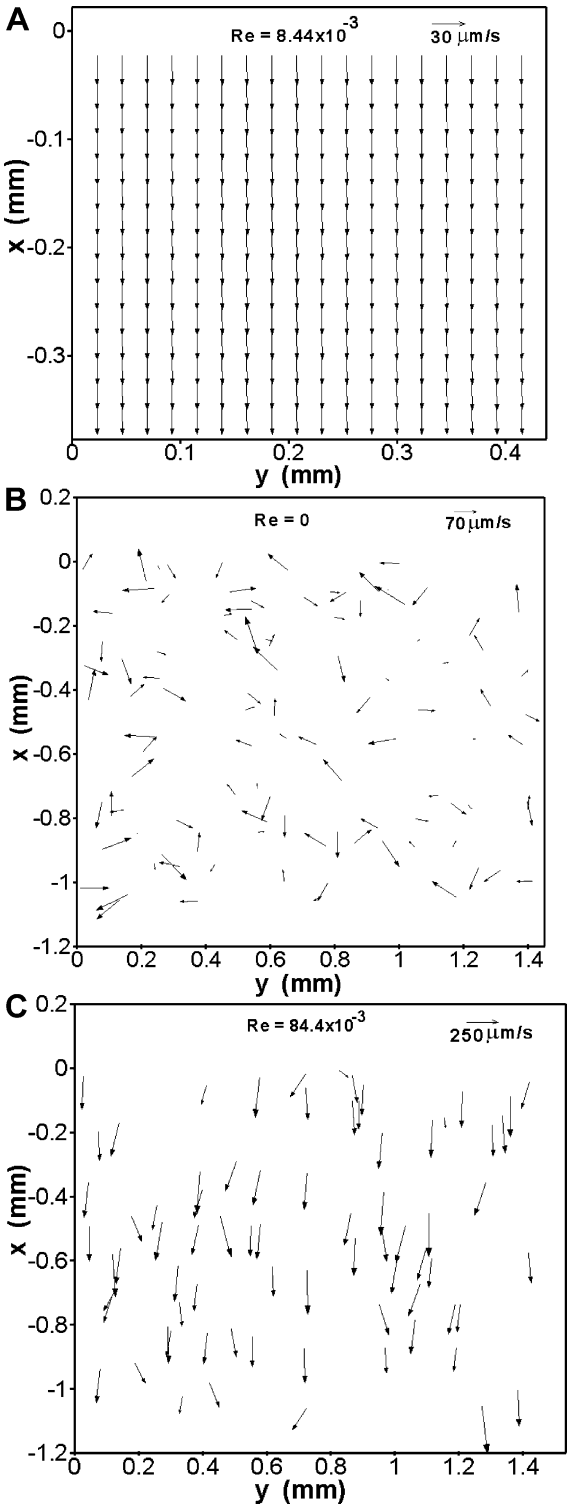

Figure 3. **A**: Vector plot of fluorescent particles observed at low flow ($Re = 8.44 \times 10^{-3}$) captured by 10X objective of microscope. The field of view is 0.42 mm × 0.4 mm. **B**: Observed vector plot of *D. primolecta* velocities in a stagnant fluid ($Re = 0$). **C**: Observed vector plot of *D. primolecta* in moving fluid ($Re = 84.4 \times 10^{-3}$) captured by 4X objective. The field of view is 1.43 mm × 1.06 mm.

flow rates as

$$v_D^- = v_{obs}^- \tag{4}$$

Different fluid flow rates (Q) that were pumped through the experimental channel were used to calculate the Reynolds number

$$Re = \frac{uL}{v} \tag{5}$$

where v is the kinematic viscosity of water ($=10^{-6}\,m^2/s$), $u = Q/A_c$ is the cross-sectionally averaged fluid flow velocity or discharge velocity in the channel, $L = 4(A_c/P_w)$ is the characteristic length, A_c is the channel cross-sectional area perpendicular to the discharge velocity, and P_w is the channel wetted perimeter. The Reynolds number is dimensionless and represents the ratio of inertial and viscous forces in a fluid flow.

The energy dissipation rates were calculated based on the following equation (Luznik et al., 2007)

$$\varepsilon(x,y) = 4v\left[\left(\frac{\partial u}{\partial x}\right)^2 + \left(\frac{\partial v}{\partial y}\right)^2 + \frac{3}{4}\left(\frac{\partial u}{\partial y}\right)^2 + \frac{3}{4}\left(\frac{\partial v}{\partial x}\right)^2 + \left(\frac{\partial u}{\partial x}\frac{\partial v}{\partial y}\right) + \frac{3}{2}\left(\frac{\partial u}{\partial y}\frac{\partial v}{\partial x}\right)\right] \tag{6}$$

Results

All experiments (PIV and PTV) showing the swimming velocities of *Dunaliella* at different fluid flow conditions are summarized in Table I. The Reynolds number in the channel ranged from $Re = 0$ in a stagnant (non-moving) fluid to $Re = 84.4 \times 10^{-3}$. Since $Re \ll 1$, fluid flow in the channel was dominated by viscous forces. The seeded fluid flow velocities (u_s) increased with the Reynolds number in the channel. All the rest of velocities with subscript "obs" refer to the observed *Dunaliella* velocities in the experimental channel. The net velocity of *Dunaliella* in the positive x-flow direction, that is, the observed velocity minus the seeded fluid flow velocity in the flow direction is denoted by u_D^+. The fluid flow energy dissipation rate (ε) over the channel cross-sectional area ranged from 10^{-8} to $10^{-5}\,m^2/s^3$. This dissipation range is customarily reported in shallow lakes, ponds, and streams.

Seeded Flow

Fluid flow rates in the experimental channel varied from zero (stagnant fluid) to $16.7 \times 10^{-11}\,m^3/s$. A vector plot of seeded velocity at low Reynolds number, $Re = 8.44 \times 10^{-3}$ in the x–y plane is depicted in Figure 3A. The plot shows unidirectional and parallel flow in the x-direction, that is, the velocity in the y-direction is minimal and hence can be neglected. The velocity that is observed at all points in the

Table I. The observed and net *D. primolecta* velocities in longitudinal (x-flow) and perpendicular (y) directions in stagnant (Re = 0) and moving fluids (Re > 0).

Flow rate, Q (10^{-11} m^3/s)	Reynolds number, Re (10^{-3})	Energy dissipation, ε (10^{-8} m^2/s^3)	Seeded velocity, u_s (μm/s)	Obs. vel. +x dir., u^+_{obs} (μm/s)	Obs. vel. −x dir., u^-_{obs} (μm/s)	Obs. vel. +y dir., v^+_{obs} (μm/s)	Obs. vel. −y dir., v^-_{obs} (μm/s)	Net Dunaliella vel. +x dir., u^+_D (μm/s)	Population statistics, $\lvert\mu_{u_D}\rvert \pm \sigma_{u_D}$ (μm/s)
Stag	0.00	0.00	0.00	41.84	39.12	36.29	35.61	41.84	2.72 ± 52.8
0.5	2.53	1.23	4.63	41.98	36.15	32.18	32.76	37.35	1.20 ± 48.2
0.83	4.22	3.43	11.26	42.24	34.59	28.58	28.8	36.79	2.20 ± 43.2
1.34	6.75	8.77	16.39	42.76	33.10	31.16	31.57	39.83	6.73 ± 44.9
1.67	8.44	13.7	20.60	43.08	32.59	25.81	25.47	41.03	8.44 ± 42.2
1.84	9.28	16.6	24.01	43.93	30.21	24.27	25.79	40.50	10.29 ± 35.2
2.00	10.13	19.7	27.07	44.96	31.81	28.24	28.17	44.47	12.66 ± 38.4
2.17	10.97	23.2	29.22	42.40	26.91	20.96	20.63	41.99	15.08 ± 31.8
2.34	11.82	26.9	35.16	48.02	33.12	30.63	30.64	48.98	15.86 ± 39.7
2.50	12.66	30.8	36.52	47.50	25.66	21.94	22.15	41.64	15.98 ± 33.4
2.67	13.5	35.1	37.23	50.69	35.73	33.35	32.99	52.35	16.62 ± 40.6
2.84	14.35	39.6	43.55	49.34	27.74	18.08	18.20	41.73	13.99 ± 28.1
3.01	15.19	44.4	47.68	50.33	33.91	33.84	33.28	45.02	11.11 ± 44.3
3.17	16.04	54.3	52.90	56.41	29.82	29.67	29.81	38.64	8.82 ± 33.1
3.34	16.88	60.2	53.62	55.20	31.99	38.40	37.06	38.65	6.66 ± 41.4
4.68	23.63	107	67.38	60.84	31.02	37.28	34.93	34.75	3.73 ± 44.9
5.84	29.54	168	89.97	87.14	39.97	29.12	29.69	41.16	1.19 ± 53.1
8.35	42.2	343	134.42	136.68	26.61	37.34	34.01	28.66	2.05 ± 68.7
11.7	59.08	672	184.39	187.86	27.52	34.00	38.27	29.65	2.13 ± 62.4
16.7	84.4	1370	276.36	273.94	53.53	43.46	35.65	57.40	3.87 ± 81.9

Note that, $u^-_{obs} = u^-_D$, $v^+_{obs} = v^+_D$, $v^-_{obs} = v^-_D$, and $u^+_D = u^+_{obs} - u_s$. μ_{u_D} and σ_{u_D} are the statistical moments of normal probability distribution. || designate an absolute value.

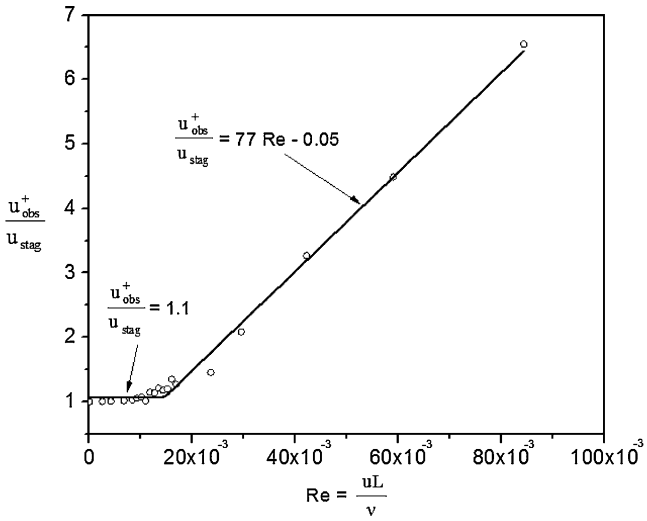

Figure 4. Ratio of observed velocities of *D. primolecta* in the positive x-flow direction (u^+_{obs}) and observed velocity of *D. primolecta* in a stagnant fluid versus Reynolds number (Re). The trend shows a constant velocity ratio for $15 \times 10^{-3} \geq Re \geq 0$ and a linear increase trend for $Re > 15 \times 10^{-3}$.

field of view of the image is almost equal to the mean velocity. Fluid flow close to the channel boundaries was not considered. The mean velocity in the field of view of Figure 3A was taken as the reference seeded velocity and was used to obtain the net velocity of *Dunaliella* in the positive x-direction.

Algal Size and Kinetics

The average size of *D. primolecta* cells observed in the experiment was approximately 11 μm for both stagnant as well as moving fluid flow conditions. Figure 2B shows the histogram plot of the diameter of *D. primolecta* cells observed in the stagnant flow. The total number of *D. primolecta* cells observed in the stagnant flow for 250 double frame images was around 47,000 and these numbers reduced with the increasing fluid flow rate. At the highest $Re = 84.4 \times 10^{-3}$, the total number of *D. primolecta* cells observed for 250 double frames was around 27,000. The swimming average velocity of *Dunaliella* in the flow direction at stagnant condition was observed to be $u_D^+ = 41.84$ μm/s and opposite to the flow direction, it was $u_D^- = 39.12$ μm/s (Table I). This shows that on average the *D. primolecta* cells swim approximately 4 times its body length per second in a stagnant fluid. Figure 3B shows the

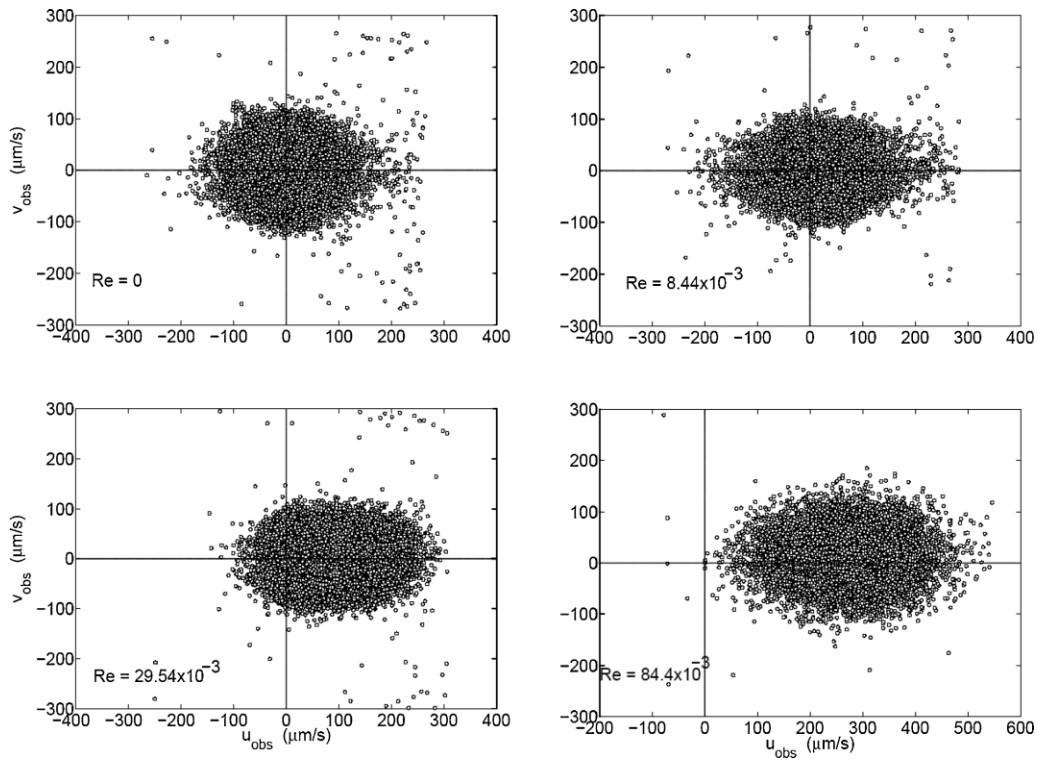

Figure 5. Scatter plot of observed *D. primolecta* velocities in the longitudinal direction (u_{obs}) and observed *Dunaliella* cells in the perpendicular direction (v_{obs}) in the channel analyzed using PTV. u_{obs} is the combined velocity of *D. primolecta* cells and the fluid flow.

vector plot of the swimming direction of *D. primolecta* cells in a stagnant fluid, $Re = 0$, and Figure 3C shows the vector plot of swimming direction in a moving fluid at $Re = 84.4 \times 10^{-3}$. While in a stagnant fluid *D. primolecta* cells move in all directions, in the moving fluid the velocity vectors of *D. primolecta* are mostly aligned in the main fluid flow direction through the channel.

The observed velocity of *D. primolecta* in the positive x-flow direction (u^{+}_{obs}) normalized with stagnant velocity (u_{stag}) when plotted against Re depicts a constant value ($u^{+}_{obs}/u_{stag} = 1.1$) for $15 \times 10^{-3} \geq Re \geq 0$ (Fig. 4). In this range of Re, *D. primolecta* cells have a control over the fluid flow in the channel. At $Re > 15 \times 10^{-3}$, *D. primolecta* cells do not have control over the fluid flow and the cells are transported in the predominant direction of fluid flow in the channel. A linear increase in the velocity ratio ($u^{+}_{obs}/u_{stag} = 77\,Re - 0.05$) is observed for $Re > 15 \times 10^{-3}$. This result demonstrates that the transport of *D. primolecta* is systematically mediated by fluid flow conditions and corresponding Re number in the channel.

Scatter Plots

The scatter plot of observed *D. primolecta* cells in the longitudinal direction of flow and observed *D. primolecta* cells in the perpendicular direction to the flow are depicted in Figure 5. It is clearly evident that at $Re = 0$ (stagnant), *D. primolecta* cells swim in all directions with almost equal velocity depicting a circular shape around the center of mass (0–0). With increase in the Re number, the center of mass is swept in the flow direction (e.g., 250–0 at $Re = 84.4 \times 10^{-3}$). Another interesting observation is the fact that net *D. primolecta* velocities are scattered all over the field of view in the micro-flow channel (around 0–0) at all Re values irrespective of the driving fluid flow velocity (Fig. 6). The scattering in all directions is also evident from the vector plot in Figure 3B and C. At maximum Reynolds number, $Re = 84.4 \times 10^{-3}$, the vector plot depicts a comparatively small velocity in the perpendicular direction of flow and indicates that *D. primolecta* was able to swim back and forth from the prevailing flow direction.

Histogram Plots

Histogram plots of the velocity of net *D. primolecta* cells for the whole sample population in the x-direction (u_D) for all flow rates depict an overall symmetric deviation around the center of mass (Fig. 7). The default null hypothesis that the *Dunaliella* velocities originate from a distribution in the normal family was successfully tested at the 5% significance

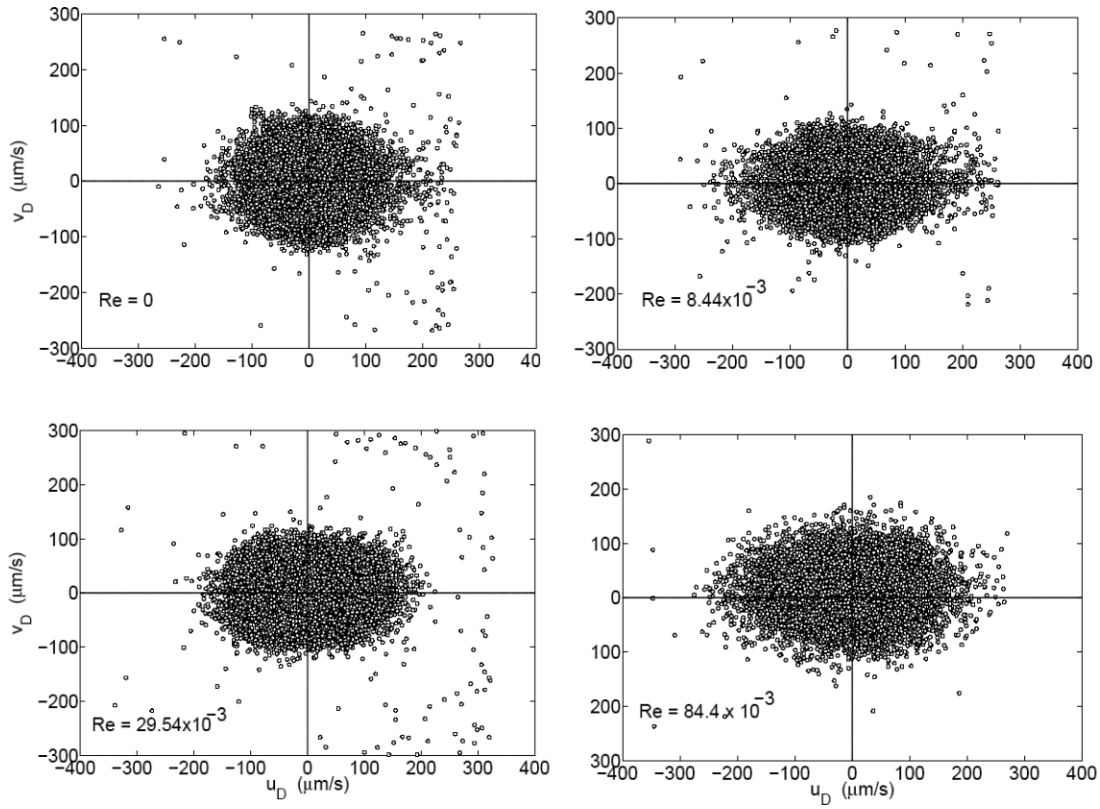

Figure 6. Scatter plot of net *D. primolecta* velocities in the longitudinal flow direction (u_D) and net *D. primolecta* cells perpendicular to the flow direction (v_D) in the channel analyzed using PTV.

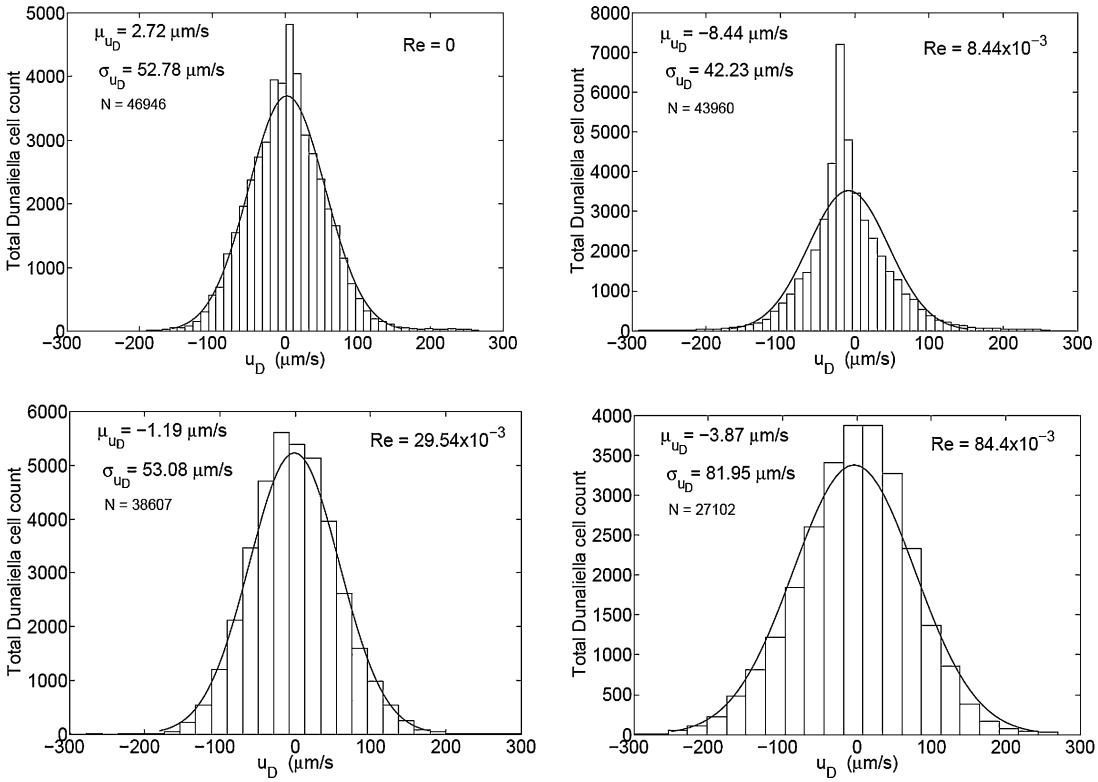

Figure 7. Histogram plot of net *D. primolecta* velocity in the longitudinal flow direction observed in the channel for 250 image pairs.

level by using the Matlab software (The MathWorks, Inc., R2008b). The first statistical moments, μ_{u_D}, of normal probability distributions of u_D were plotted versus corresponding Reynolds numbers in Figure 8. The sample population mean velocities follow a log-normal distribution with $R^2 = 0.95$. Reynolds number at maximum mean velocity ratio, $\mu_{u_D}/\mu_{u\,stag} \approx 6$, was $Re_c = 13 \times 10^{-3}$. The net sample population velocity of *D. primolecta* was two times larger than the corresponding velocity in a stagnant fluid in the approximate range of $17 \times 10^{-3} > Re > 8 \times 10^{-3}$. Outside of this range, *D. primolecta* velocities were not systematically affected by moving fluid. The second statistical moments, σ_{u_D}, were plotted versus Reynolds number in Figure 9. The plot depicts that the σ_{u_D} decreases in the range of $15 \times 10^{-3} \geq Re \geq 0$ with a minimum close to $\sigma_{u_D} \sim 28\ \mu m/s$ at $Re \approx 15 \times 10^{-3}$. At $84 \times 10^{-3} > Re > 15 \times 10^{-3}$, σ_{u_D} increases up to 82 μm/s at the highest Re. The values of σ_{u_D} are typical for the reported in situ velocity measurements of microorganisms (Sheng et al., 2007). The results demonstrate a significant effect of local fluid flow velocities on the variability of *D. primolecta* velocities.

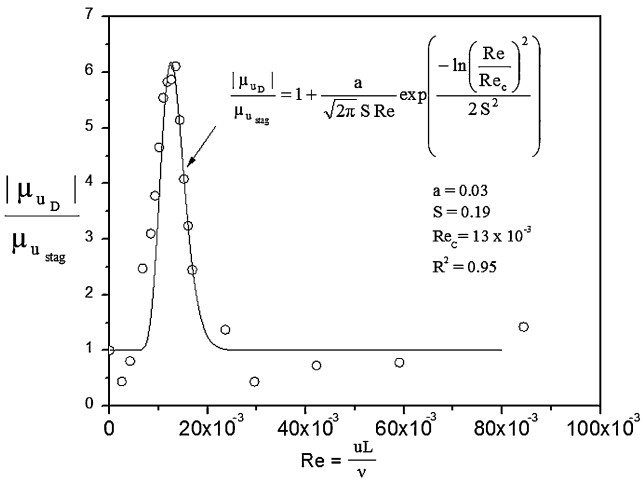

Figure 8. Ratio of sample population velocities of *D. primolecta* in the positive x-flow direction (μ_{u_D}) and population velocity in a stagnant fluid ($\mu_{u_{stag}}$) versus Reynolds number (Re).

Discussion

Under field conditions algal cells could be subjected to a variety of fluid motions starting with the large scale eddies, usually determined by the geometry of aquatic environment, for example, water depth, down to smallest eddies on the order of a millimeter where as the kinetic energy is converted into heat by the action of molecular viscosity (Hondzo and

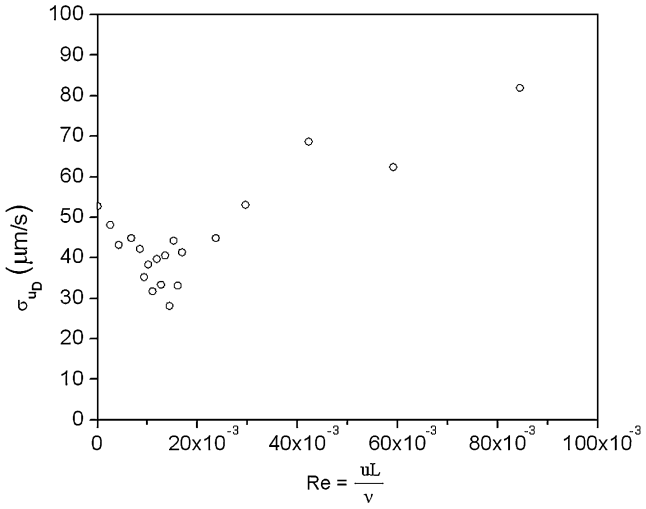

Figure 9. Standard deviation plot of *D. primolecta* sample population velocities in the longitudinal flow direction (σ_{u_D}) observed in the channel.

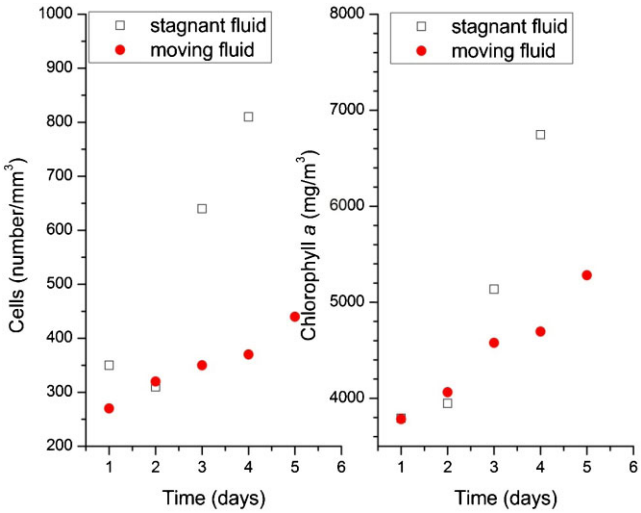

Figure 10. *D. primolecta* accrual in a stagnant fluid (Re = 0) and in the moving fluid with an average fluid flow energy dissipation rate $\varepsilon \approx 10^{-6}$ m^2/s^3. Experiments were conducted in a 35 L bioreactor. [Color figure can be seen in the online version of this article, available at www.interscience.wiley.com.]

Wüest, 2009). Our results demonstrate that the kinetics of *Dunaliella* cells is mediated by local fluid flow conditions. This implies that *Dunaliella* cells are imbedded in the large range of eddies that transport *Dunaliella* cells through a variety of nutrient concentrations and associated photosynthetically active radiation levels in aquatic environments. At the scale of individual *Dunaliella* cell (about 10 μm), the cell is exposed to a velocity gradient that is the ultimate consequence of large scale eddies in aquatic ecosystems. The velocity gradients at the cell scale are determined by energy dissipation level. We employed micro-PIV to systematically change the velocity gradients in the proximity of *Dunaliella* cells. The velocity gradients generated in the channel resulted in the energy dissipation range from $\varepsilon = 10^{-8}$ to 10^{-5} m^2/s^3 (Table I). These energy dissipation rates are commonly observed in the surface layers of shallow lakes and ponds in aquatic ecosystems (Hondzo and Warnaars, 2008). This implies that our laboratory measurements should be scalable or transferable to field conditions.

Our experiments demonstrate that small scale velocity gradients modulate kinematic responses of a motile and bi-flagellated green alga. To what extent the small scale velocity gradients modulate the physiological responses of *Dunaliella* is unknown. In order to facilitate the question, we conducted a preliminary experiment in a 35 L bioreactor with controllable small scale velocity gradients (Warnaars et al., 2006). Two independent experiments under identical nutrients, temperature, and light conditions were conducted under stagnant fluid (Re = 0 in this study) and in a moving fluid with $\varepsilon \approx 10^{-6}$ m^2/s^3 (Re $\approx 23.6 \times 10^{-3}$ in this study). A twofold increase in *D. primolecta* number and chlorophyll-a concentrations were observed in a stagnant fluid in comparison to the moving fluid at day 5 after the initiation of experiment (Fig. 10). While small scale velocity gradients facilitate the accrual of unicellular non-motile green algae *Selenastrum capricornutum* (e.g., Warnaars and Hondzo, 2006), the accrual of *D. primolecta* was inhibited by the moving fluid. In order to provide algal cells photosynthetically active radiation in bioreactors, mechanical mixers are often employed. The induced velocity gradients by the mixers will influence the kinetic responses of *Dunaliella* and very likely may have an effect on algal physiology. The experiments reported in this study could be instrumental in the design of efficient bioreactors for the harvest of *Dunaliella*.

Nomenclature

A_c	area of micro flow channel
Q	flow rate or discharge pumped into the flow channel
P_w	flow channel wetted perimeter
u	discharge velocity in the flow channel
v	kinematic viscosity of water at room temperature
u_{obs}	observed *Dunaliella* velocity in longitudinal direction
u^+_{obs}	observed *Dunaliella* velocity in the positive x-flow (longitudinal) direction
u^-_{obs}	observed *Dunaliella* velocity opposite to the x-flow (longitudinal) direction
u_D	net velocity of *Dunaliella* cells in the longitudinal (x-flow) direction
u_s	seeded flow velocity
u_{stage}	stagnant *Dunaliella* velocity
v_{obs}	observed *Dunaliella* velocity in the perpendicular direction
v^+_{obs}	observed *Dunaliella* velocity perpendicular to the flow in the positive y–flow direction
v^-_{obs}	observed *Dunaliella* velocity perpendicular to the flow in the negative y–flow direction
v_D	net velocity of *Dunaliella* velocity in the perpendicular (y) direction

μ_{u_D} the first statistical moment (mean) of normal probability distribution of u_D in the longitudinal flow direction

σ_{u_D} the second statistical moment of normal probability distribution of u_D in the longitudinal flow direction

$|\,|$ designate an absolute value

The authors are grateful to technical support and assistance at the *Chlamydomonas* Center, Department of Plant Biology, University of Minnesota. This work was partially supported by the National Center for Earth-surface Dynamics (NCED), a Science and Technology Center funded by the Office of Integrative Activities of the National Science Foundation under agreement EAR-0120914. Additional financial support was provided by the Minnesota Futures Grant, 2009, University of Minnesota.

References

Agarwal GP. 1990. Glycerol. Adv Biochem Eng/Biotechnol 41:95–125.

Aizawa K, Miyachi S., 1992. Photosynthesis: Biochemical and physiological and adaptation. In: Avron M, Ben-Amotz A, editors. Dunaliella: Physiology, biochemistry, and biotechnology. Florida: CRC Press. p. 45–62.

Avron M., 1992. Osmoregulation. In: Avron M, Ben-Amotz A, editors. Dunaliella: Physiology, biochemistry, and biotechnology. Florida: CRC Press. p. 135–164.

Ben-Amotz A. 1980. Glycerol, β-carotene and dry algal meal production by commercial cultivation of Dunaliella. In: Shelef G, Soeder CJ, editors. Algae biomass, production and use. Amsterdam: Elsevier. p. 603–610.

Ben-Amotz A, Avron M., 1982. Glycerol and β-carotene metabolism in the halotolerant alga Dunaliella: A model system for biosolar energy conversion. Trends Biochem Sci 6:297–299.

Ben-Amotz A Sussman I Avron M 1982 Glycerol production by *Dunaliella* Experientia 38:49–52.

Ben-Amotz A, Shaish A, Avron M. 1991. The biotechnology of cultivating *Dunaliella* for production of β-carotene rich algae. Bioresour Technol 38:233–235.

Borowitzka LJ, Borowitzka MA, Moulton TP. 1984. The mass-culture of Dunaliella Salina for fine chemicals-from laboratory to pilot plant. Hydrobiologia 116:115–121.

Chen H, Jiang JG. 2009. Osmotic responses of Dunaliella to the changes of salinity. J Cell Physiol 219:251–258.

Chisti Y. 2007. Biodiesel from microalgae. Biotechnol Adv 25:294–306.

Cowan AK, Rose PD, Horne LG. 1992. Dunaliella salina: A model system for studying the response of plant cells to stress. J Exp Bot 43:1535–1547.

EIO:. 1999. International Energy Outlook, Washington, DC, US Department of Energy, Energy Information Administration, DOE/EIA-0484.

Gouveia L, Oliveira AC. 2009. Microalgae as a raw material for biofuels production. J Ind Microbiol Biotechnol 36:269–274.

Hadi MR, Shariati M, Afsharzadeh S. 2008. Microalgal biotechnology: Carotenoid and glycerol production by the green algae Dunaliella isolated from the Gave-Khooni Salt Marsh, Iran. Biotechnol Bioprocess Eng 13:540–544.

Haghjou MM, Shariati M, Smirnoff N. 2009. The effect of acute high light and low temperature stress on the ascorbate-glutathione cycle and superoxide dismutase activity in two Dunaliella salina strains. Physiologia Plantarum 135:272–280.

Hejazi MA, Wijffels RH. 2003. Effect of light intensity on beta-carotene production and extraction by *Dunaliella salina* in twophase bioreactors. Biomol Eng 20:171–175.

Hieber AD, King TJ, Morioka S, Fukushima LH, Franke AA, Bertram JS. 2000. Comparative effects of all-trans beta-carotene vs. 9-*cis* beta-carotene on carcinogen-induced neoplastic transformation and connexin 43 expression in murine 10T1/2 cells and on the differentiation of human keratinocytes. Nutr Cancer 37:234–244.

Hondzo M, Warnaars TA. 2008. Coupled effects of small-scale turbulence and phytoplankton biomass in a small stratified lake. J Environ Eng 134:954–960.

Hondzo M, Wüest A. 2009. Do microscopic organisms feel turbulent flows? Environ Sci Technol 43:764–768.

Jin E, Melis A. 2003. Microalgal biotechnology: Carotenoid production by the green algae Dunaliella salina. Biotechnol Bioprocess Eng 8:331–337.

Lamers PP, Janssen M, De Vos RCH, Bino RJ, Wijffels RH. 2008. Exploring and exploiting carotenoid accumulation in *Dunaliella salina* for cell-factory applications. Trends Biotechnol 26:631–638.

Loeblich LA. 1974. Action spectra and effect of light intensity on growth pigments and photosynthesis in Dunaliella Salina. J Protozool 21:420–425.

Luznik L, Gurka R, Nimmo Smith WAM, Zhu W, Katz J, Osborn TR. 2007. Distribution of energy spectra, Reynolds stresses, turbulence production and dissipation in a tidally driven bottom boundary layer. J Phys Oceanogr 37:1527–1550.

Meinhart CD, Wereley ST, Santiago JG. 1999. PIV measurements of a microchannel flow. Exp Fluids 27:414–419.

Mishra A, Mandoli A, Jha B. 2008. Physiological characterization and stress-induced metabolic responses of *Dunaliella salina* isolated from salt pan. J Ind Microbiol Biotechnol 35:1093–1101.

Raja R, Hemaiswarya S, Rengasamy R. 2007. Exploitation of Dunaliella for β-carotene production. Appl Microbiol Biotechnol 74:517–523.

Santiago JG, Wereley ST, Meinhart CD, Beebe DJ, Adrian RJ. 1998. A particle image velocimetry system for microfluidics. Exp Fluids 25:316–319.

Schlipalius L. 1991. The extensive commercial cultivation of *Dunaliella salina*. Bioresour Technol 38:241–243.

Sheng J, Malkiel E, Katz J, Adolf J, Belas R. 2007. Digital holographic microscopy reveals prey-induced changes in swimming behavior of predatory dinoflagellates. Proc Natl Acad Sci USA 104:17512–17517.

Thakur A, Kumar HD. 1998. Glycerol production by *Dunaliella salina* in response to various combinations of organic carbon compounds. Cytobios 93:129–134.

Thakur A, Kumar HD, Cowsik SM. 2000. Effect of pH and inorganic carbon concentration on growth, glycerol production, photosynthesis and dark respiration of Dunaliella salina. Cytobios 102:69–74.

Tompkins J, DeVille MM, Day JG, Turner MF. 1995. Culture collection of algae and protozoa: Catalogue of strains. Kendal, UK: Titus Wilson and Sons Ltd. 203. pp.

Tornabene TG, Holzer G, Peterson SL. 1980. Lipid profile of the halophilic alga, Dunaliella Salina. Biochem Biophys Res Commun 96:1349–1356.

Vanitha A, Narayan MS, Murthy KNC, Ravishankar GA. 2007. Comparative study of lipid composition of two halotolerant alga, Dunaliella bardawil and Dunaliella salina. Int J Food Sci Nutr 58:373–382.

Warnaars T, Hondzo M. 2006. Small-scale fluid motion mediates growth and nutrient uptake rate of *Selenastrum capricornutum*. Freshwater Biol 51:999–1015.

Warnaars T, Hondzo M, Carper MA. 2006. A desktop apparatus for studying interactions between microorganisms and small-scale fluid motion. Hydrobiologia 563:431–443.

Zhu YH, Jiang JG. 2008. Continuous cultivation of Dunaliella salina in photobioreactor for the production of beta-carotene. Eur Food Res Technol 227:953–959.